Ab Initio Molecular Dynamics Study of the Hydration of a Sodium Smectite Clay

E. S. Boek*

Schlumberger Cambridge Research, High Cross, Madingley Road, Cambridge CB3 0EL, United Kingdom

M. Sprik

Department of Chemistry, University of Cambridge, Cambridge CB2 1EW, United Kingdom

Received: June 7, 2002; In Final Form: January 3, 2003

Ab Initio molecular dynamics simulations have been performed to study the hydration of a sodium smectite clay. Water molecules are intercalated as a double layer in the interlayer spacing of this swelling clay mineral. The solvent structure was found to be very similar to predictions by a previous Monte Carlo study based on classical pair potentials (Boek, E. S.; Coveney, P. V.; Skipper, N. T. *J. Am. Chem. Soc.* **1995**, *117*, 12608). This lends support to our observations regarding the dynamics of the water molecules. First, the water shows a strong preference to form a hydrogen-bonded network between the solvent molecules. The hydrogen bonds to the aluminosilicate surface are only weak and short-lived. Second, the solvent displays liquidlike relaxation dynamics. Our results suggest that, because of the two-surface geometry in clays, intercalated water is prevented from freezing and should be considered in terms of a confined liquid. This is consistent with recent QENS experiments. Finally, we have calculated the power spectra for both hydrated and dehydrated clay from a Fourier transform of the MD trajectories. The calculated spectra are compared with experimental FTIR spectra.

I. Introduction

Clay swelling is a process that plays a key role in many industrial processes such as catalysis and drilling for hydrocarbons. To understand swelling behavior, detailed knowledge of water adsorption on clay surfaces is crucial as well as knowledge of the hydration of counterions in the clay interlayer spacing. Montmorillonites have frequently been used as model systems for the study of these effects both in experiment[1] and modeling.[2−9] These (relatively simple) natural smectite clays occur as micrometer-sized particles in many soils and sediments.[10] They are mined commercially and have many practical applications.[1] For example, they are used widely in drilling fluids and as semipermeable barriers to organic and radioactive wastes. Among montmorillonites, the sodium intercalates are the archetypal swelling clay minerals. They are composed of negatively charged pyrophyllitelike sheets that are held together by charge-balancing sodium cations.[11] In humid atmospheres, these interlayer sodium ions have a strong tendency to hydrate, thereby increasing the clay layer spacing. This process is known as crystalline swelling. Further expansion takes place when the clays are immersed in liquid water. This process is known as macroscopic swelling and leads to the formation of colloidal suspensions.[10,12,13]

The hydration of Na−, K−, and Li−montmorillonite clays has been the subject of a number of force field-based Monte Carlo (MC)[4−6] and molecular dynamics (MD)[7,14] studies. These investigations showed that pairwise additive atomistic models are capable of reproducing the equilibrium swelling behavior of real clays. However, a very careful tuning of the pair potentials is required to achieve this.[5] The question of which interaction potential to choose for hydrated smectite clays with different counterions is still a matter of hot debate.[5,7,14,15]

One way to avoid such problems is through the use of ab initio molecular dynamics (AIMD).[18] The atomic forces in this scheme are obtained from a continuously updated electronic structure calculation. The electronic structure calculation is based on the density functional theory (DFT) for periodic extended systems as originally developed for application to solids. Because of the coupling to MD, the finite-temperature ionic dynamics is also described by this technique, opening up the modeling of liquids to electronic structure methods. This enables us to account for the presence of the aqueous solvent in a manner that is similar to that used in classical simulation. A definite advantage of the ab initio MD approach over previous modeling studies[5,6,14,16] is that the constraint of rigid clay platelets, needed to stabilize the solid framework, can be eliminated. This brings the relaxation of the crystal geometry and the vibrational dynamics of the mineral layers within reach of detailed theoretical investigation.

The interactions of clay and related mica surfaces with water and other adsorbates have already been addressed using similar plane wave pseudopotential-based DFT methods. Recently, this methodology was applied to the intercalation and polymerization of organic molecules within the clay interlayer spacing.[17] The dynamics of the water was, however, not taken into consideration by this study. Similarly, an earlier ab initio MD study of water adsorption at the surface of muscovite mica found that water condensed into an essentially crystalline fully connected 2D hydrogen bond network, denoted as 2D ice.[19] Water in swelling clays, on the contrary, is not frozen. This was recently demonstrated experimentally by quasi-elastic neutron scattering (QENS) of water in a vermiculite clay.[20] Note that vermiculites have hydration properties that are very similar to those of smectites.[21]

The first objective of the present ab initio MD simulation is, therefore, the verification of this crucial result without the uncertainties of the parametrization of force fields, as used in

* Corresponding author. E-mail: boek@cambridge.oilfield.slb.com.

10.1021/jp0262564 CCC: $25.00
Published on Web 03/19/2003

the classical MD simulations mentioned above.[7,14] Anticipating our results, we find that water adsorbed in the interlayer spacing of our model clay behaves like a confined fluid. The mineral layer remained stable in the course of our simulation, keeping an average structure close to the experimental structure. The dynamical fluctuations of the silicon and oxygen atoms in the tetrahedral layer were converted into vibrational densities of states. The resulting spectra for hydrated and completely dehydrated clays were compared. The motivation behind this comparison is to help resolve the question of whether infrared spectroscopy can be used as an in situ probe of the degree of hydration of clays encountered in oil exploration, as suggested in ref 22. The organization of the paper is as follows. First, the clay simulation model and the ab initio MD method will be outlined. We then report on the simulation results.

II. Clay Simulation Model

The size of unit cells of complex minerals such as clays often exceeds the limit of what can conveniently be treated by current ab initio MD methods. Simplifications, sometimes fairly drastic, are therefore inevitable. In this section, our particular choice of model system will be discussed and justified. The basis is the model Wyoming montmorillonite (belonging to the smectite family of clay minerals[10]) used in our classical Monte Carlo simulations.[5] This is a 2:1 layered dioctahedral aluminosilicate[10] with the unit-cell formula

$$Na_{0.75}nH_2O[Si_{7.75}Al_{0.25}][Al_{3.5}Mg_{0.5}]O_{20}(OH)_4 \qquad (1)$$

Layers of octahedrally coordinated Al^{3+} ions are sandwiched between sheets of tetrahedral silicate units. The vertices are pointing toward the octahedral layer. The basal planes of the tetrahedra form distorted hexagonal rings. For typical Wyoming-type montmorillonite,[10] the aluminum in the octahedral layer is substituted by Mg with a ratio of 1:8. In the tetrahedral network, 1 out of 32 Si ions is substituted by Al. These substitutions give rise to an overall negative charge on the clay framework. This negative charge is balanced by the sodium counterions.

The classical simulation cells of ref 5 were made up of eight of the unit cells[5] defined by eq 1 containing a total of six sodium cations. For the ab initio MD calculations, these numbers were reduced to two unit cells and one Na^+ ion, which compensates for one isomorphic substitution in the clay framework. For the substitution site, we chose a Si in the tetrahedral layer that was replaced by Al. Whereas this composition amounts to a slightly higher fraction of charged sites, it still approximately maintains the charge density on the clay platelet as in eq 1, which is typical for smectite clay.[23,24] The rationale for preferring a tetrahedral over an octahedral substitution is that, according to the accepted picture of charge density in clays, the negative charge associated with the tetrahedral substitution is distributed over just the three surface oxygens of one tetrahedron. The resulting defect structure is therefore more localized as compared with its octahedral counterpart[23] and, presumably, less affected by the periodic boundary conditions in our small system. Note that we have checked finite size effects by performing a MC force field simulation for the clay model size described above. It appears that the MC simulations yield approximately the same results for both the 8- and 2-unit-cell models. This will be discussed in section IV.B. Therefore, we feel that it is justified to use the 2-unit-cell system size in the current ab initio simulations.

The next question concerns the quantity of water to be included (n in eq 1). Our guide here was again the experience from the model calculation of ref 5. It was found that inserting 64 waters into the 8-unit-cell system was just sufficient for the creation of a water double layer, increasing the interlayer spacing from 10.2 Å for dehydrated (dry) clay to 15.1 Å. This expansion of 4.9 Å is in excellent agreement with experiment.[5] Keeping the same ratio and dimensions along the vertical (c) axis, we added $n = 16$ water molecules to our 2-unit-cell system. In summary, our simulation box has the following unit-cell formula:

$$Na_{1.00}16H_2O[Si_{31}Al_1][Al_8]O_{40}(OH)_8 \qquad (2)$$

This corresponds with a clay sheet of 10.56 Å × 9.14 Å. The thickness of one clay layer is 6.56 Å. The clay with a double layer of water has a thickness of 15.01 Å. We also consider a dehydrated clay with a layer spacing of 10.17 Å. This system was replicated in all three directions by periodic boundary conditions. We are therefore simulating 3D particles of clay, as would occur in nature, rather than two sheets in isolation.

III. Ab Initio MD Method

Electronic structures were computed using a plane wave pseudopotential implementation of Kohn−Sham DFT. The calculations are based on the BLYP energy functional. This functional consists of the exchange contribution by Becke[25] and a correlation term according to Lee−Yang−Parr.[26] Kohn−Sham orbitals are expanded in plane waves up to an energy cutoff of 70 Ry in combination with medium-soft norm-conserving pseudopotentials according to the Troullier−Martins (TM) scheme.[27] (Details of the pseudopotentials can be found in the Appendix.) The equations of motion for ions and orbitals were integrated using a fictitious electron mass of 1000 au and a time step of 7 au (0.169 fs). The temperature was maintained at an average of 300 K.

This or a comparable setup has been validated by a growing number of ab initio MD studies of aqueous systems. A key observation is that the structure of the local environment and the self-diffusion coefficient, two critical parameters for the hydrogen bonding in water, can be reproduced with sufficient accuracy provided an appropriate density functional is used.[28−31] Among these functionals, the BLYP generalized gradient approximation (GGA) was found to give the most consistent performance.[28,29] The same functional has been the basis of the majority of computational studies of aqueous solutions with mostly satisfying results. In view of the relevance to the present clay calculation, we mention here the gas-phase hydration and bulk solvation of Li^+,[32] Na^+,[33,34] K^+,[35] Be^{2+},[36] Ca^{2+},[37] ammonium,[38] and aluminum hydroxide.[39] Also, the solvation of aqueous anions, which is perhaps a more critical test, is described to be in fair agreement with experiment. (For chlorides, see refs 40−42, and for fluorides, ref 43.)

Examples of successful applications to mineral systems can be found in refs 19 and 44−46. In particular, this scheme has resulted in good agreement between theoretical and experimental features of bulk muscovite.[19] There is, therefore, good reason to expect a similar performance for the description of hydrogen bond formation and polarization effects at the smectite−water interface during clay hydration.

All calculations were carried out using the CPMD package.[47] As a starting point, we used a sample from the equilibrated Monte Carlo simulations of ref 5 that was adapted to fit the smaller periodicity of the cell. The wave function and geometry were optimized, and the result served as the initial configuration for the MD simulations. After equilibration, the MD run was

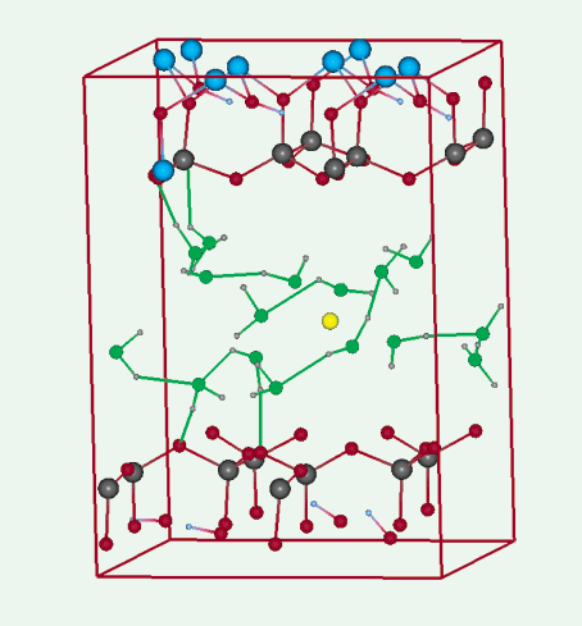

Figure 1. Snapshot of a clay hydrate simulation. The simulation cell contains two unit cells. This corresponds to a total of 64 O, 9 Al, 15 Si, 40 H atoms, and 1 Na^+ ion.

continued for a period of 1 ps for both the wet and the dry clay. This rather short time window is just long enough to observe the reorientational motion distinguishing liquid water from ice. A simulation snapshot is shown in Figure 1.

IV. Results and Discussion

A. Counterion Adsorption Energies. To validate our density functional approach and to set a benchmark for future comparison, we calculated the relative adsorption energies of sodium ions in three different adsorption sites on the dehydrated clay by means of geometry optimization. The sodium ions were released at positions above the Al tetrahedron—the Si_5Al and Si_6 rings. The initial distance between the ion and the surface oxygens was approximately 3 Å. The results are as follows. The sodium ion is more strongly bound to the Si_5Al ring than to the Si_6 ring by 14 kJ/mol. This modest enhancement suggests that charge localization on oxygens directly connected to the substitution site is a relatively minor effect. The competing position above the Al tetrahedron is higher in energy by 43 kJ/mol. These values are in qualitative agreement with those in ref 19.

B. Solvent Structure. A vital piece of information to the understanding of clay swelling is the degree of hydration of the bentonite surface compared with that of the counterion. To characterize the structure of the confined aqueous system, we determined radial distribution functions (RDF) and density profiles perpendicular to the clay surface.

The RDFs were determined for pairs of water oxygens, water hydrogens, clay oxygens, and sodium ions. The results are shown in Figure 2. The positions of the first peaks of these RDFs as well as the coordination numbers for the first solvation shell (and second shell for O_c-H_w) are compared in Table 1 to the model potential calculations of ref 5. Despite the substantial differences in computational approach, the ab initio MD and MC give a very similar solvent structures. The simulated coordination number of Na^+ of about 5 and the average Na^+-O distance of 2.37 Å are also consistent with experimental data.[48]

On the basis of the validation results for the RDFs, we now determine the density profiles perpendicular to the clay surface.

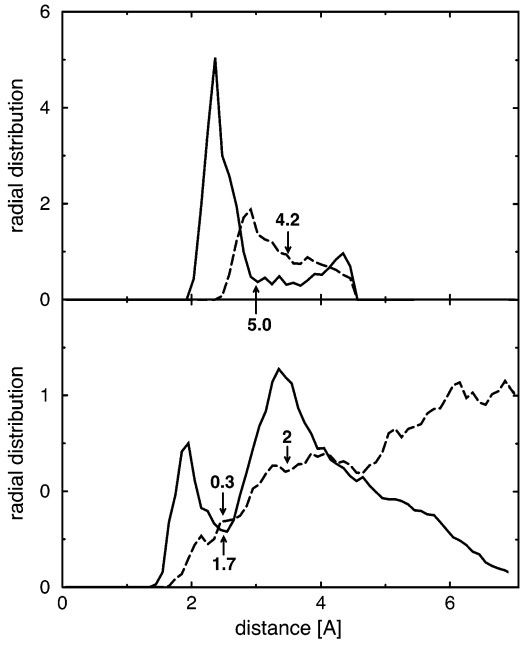

Figure 2. Radial distribution functions (RDFs) for water oxygen (O_w), water hydrogen (H_w), clay oxygen (O_c), and Na^+. The top graph shows the RDFs for O_w-O_w (− −) and Na^+-O_w (—). The bottom graph shows the RDFs for O_w-H_w (—) and O_c-H_w (− −). The numbers indicate the first-shell coordination numbers. The normalization of the RDFs is relative to the value of the O_w-O_w RDF at $r = 3.5$ Å.

TABLE 1: Position of the First Peak in RDFs and Coordination Number of the First Shell (and Second Shell for O_c-H_w) Compared for the ab Initio Molecular Dynamics (AIMD) and Classical MC Results[5] [a]

	first peak in $g(r)$ (Å)		coordination no.			
	AIMD	MC	AIMD		MC	
$Na-O_w$	2.37	2.30	5.0		5.0	
O_w-O_w	2.92	2.80	4.2		4.4	
O_w-H_w	1.9	1.80	1.7		1.6	
O_c-H_w	2.14	1.90	0.3	2	0.3	2.7

[a] The notation is the same as that used in Figure 2.

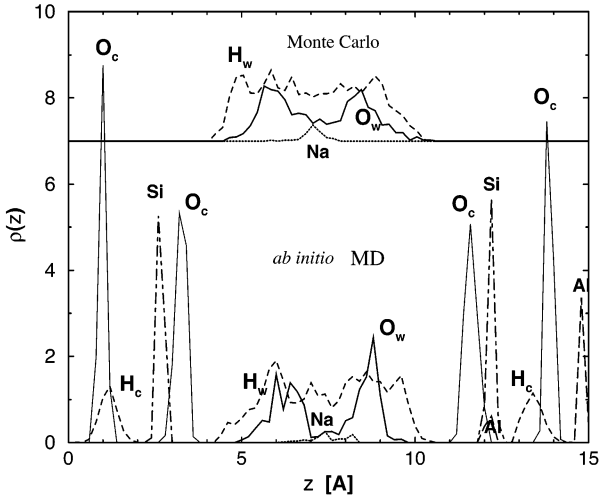

Figure 3. Density profiles for clay layer species (Si, Al, clay oxygen O_c, and clay hydrogen H_c) and interlayer species (water oxygen O_w (—), water hydrogen H_w (− −), and Na^+ (- -)). At the top, we present the profiles resulting from a MC force field simulation using the same clay cell system size.

The density profiles are shown in Figure 3. Note that these profiles have not been obtained by reflection of the data about

the layer midplane at 7.5 Å because the symmetry of the system is broken by the substitution of one Si by Al in the top tetrahedral clay layer. In the following, the position of the peaks in the top layer, represented for convenience as if reflected about the midplane at 7.5 Å, will be given in brackets. The sharp peaks at 15.0, 1.1 (1.1), 2.7 (2.8), and 3.4 (3.4) Å correspond to octahedral Al and O and to Si and surface (tetrahedral) O atoms in the clay layer, respectively. These positions are consistent with experimental neutron-diffraction density profiles of a hydrated vermiculite.[21] Note that we do not observe water adsorbed in the hexagonal cavity sites for 1.5 Å $< z <$ 4.0 Å, as was found experimentally in the case of vermiculite.[21] This may be due to the fact that vermiculite is a trioctahedral clay mineral with a higher surface-charge density than smectite.[10] Note also that the differences between top- and bottom-layer positions are negligible for the peaks considered. A significant difference, however, is found for the hydrogen atoms of the hydroxyl groups in the clay sheet, which show a broad peak around 1.3 Å in the bottom layer compared with 1.6 Å in the top layer (after reflection). This is probably due to the presence of the Al substitution, at 12.2 Å (unreflected), in the top tetrahedral layer. In this context, it is interesting to compare the smectite hydroxyl H peak values of 1.3 (1.6) Å with the value of 2.1 Å for vermiculite, where the OH layer bond is normal to the clay surface.[12] Because the smectite OH groups are less exposed at the clay surface, it may be speculated that these OH groups give rise to a less acidic[10] and less reactive clay surface than their vermiculite counterparts.

The interlayer structure is characterized by a water oxygen peak at 6.0 (6.2) Å and water H peaks at 5.3 (5.3) and 6.0 (6.4) Å. In the case of vermiculite, the hydrogen bonding between water and the clay surface was more pronounced,[21] possibly due again to the higher vermiculite surface charge density. According to our simulations, the Na^+ ions are located around the midplane at 7.5 Å. X-ray diffraction data of vermiculite hydrates[49] are consistent with this observation. Although neutron experiments cannot distinguish sodium ions from oxygen, the small peak centered on the midplane is probably due to the Na^+ ions.[21] However, this observation is at odds with classical MD simulations,[7,14] which show that the ions are partitioned in an inner-sphere surface complex (related to the tetrahedral substitution site) and an outer-sphere complex in the interlayer midplane.[23] Note that the simulation was begun with the cation in the midplane and that the simulation time may not have been sufficient to capture the speciation effect between inner- and outer-sphere surface complexes.[23] Further systematic simulation studies are required to resolve this issue.

To justify the use of our 2-unit-cell clay model, we have performed a MC force field calculation for the same system size. First, we note that the resulting layer spacing (14.85 ± 0.34) Å from constant (*NpT*) simulations of the small model is, within the error margin, identical to the one reported for the large (8-cell) system (14.96 ± 0.09).[5] Second, we note that the density profiles of the water oxygens and hydrogens as well as the sodium ion are very similar to the ones obtained from the ab initio MD simulations. (See Figure 3.)

As can be inferred from the nearest-neighbor coordination (Table 1), the number of hydrogen bonds formed between water and clay is much smaller than the number between the water molecules themselves. This is in good agreement with recent results from FTIR experiments of bentonite surface hydration,[22] showing little evidence for hydrogen bonding between water and the bentonite surface. Evidently, contrary to the icelike layers adsorbed on the mica system of ref 19 and other oxide surfaces, the solvent oxygen atoms prevail in the competition for hydrogen bonds when confined between the two interfaces in the clay. The constraints of the clay geometry also have a distinctly different effect on the dynamics: using graphical animation techniques, we could clearly observe the typical solvent reorientational and translational motion encountered in the liquid state, indicating that the water double layer is not frozen. Unfortunately, the duration of our run is too short for a quantitative determination of the self-diffusion coefficient and rotational relaxation times. In the QENS experiments of water in vermiculite clay[20] mentioned above, the correlation time of the rotational motion of water was estimated to be ∼27 ps. Although this time scale cannot yet be accessed by ab initio MD simulations because of computational limitations, animation using molecular graphics software suggests that the reorientation times in our model are likely to be shorter.

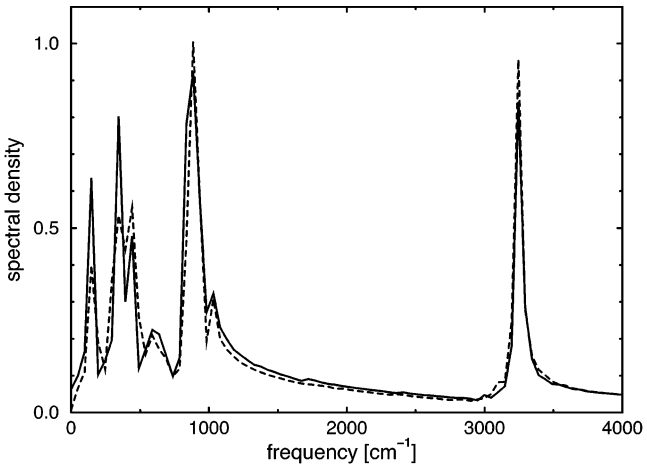

Figure 4. Hydrogen power spectra of hydrated clay (—) and dry clay (– –) systems.

C. Vibrational Dynamics. Recently, experimental FTIR work has been carried out to investigate the surface hydration process on bentonite.[22] Significant differences in the silicate ν-(Si−O) stretching region were found between the spectra of "dry" bentonite powder (with its natural water content) and a wet bentonite film. The IR spectrum of a wet bentonite film exhibits absorption bands at 1086 and 1018 cm^{-1} that disappear upon drying. These results were explained in terms of the formation of an extended electrical double layer between the platelets.

Here we calculate power spectra from the MD trajectories by means of a Fourier transform of the atomic velocity autocorrelation functions of selected atomic species. In Figure 4, the clay hydrogen spectra are shown for both the wet and dry clay. The HO stretching mode can be identified at 3630 cm^{-1}, in agreement with experiment.[12] A further signature of the experimental clay spectra can also be easily recognized in the simulated spectrum; namely, the absorption by the HO bending mode of the Al_2OH groups absorb near 920 cm^{-1},[53] providing further support for our method. (The DFT frequencies have a tendency to be too low. The underestimation can be as much as 15%.)

The vibrational motion of interest is the Si−O bond stretching. Figure 5 gives the results for the vibrational density of states as obtained from the Si and bonded O atom dynamics for both the wet and dry clay systems. It can be seen that the silicate ν(Si−O) stretching region of the wet clay has a more pronounced profile compared to that of the dry clay. This seems to contradict the experimental data.[22] However, for an assessment of this negative result, it should be pointed out that,

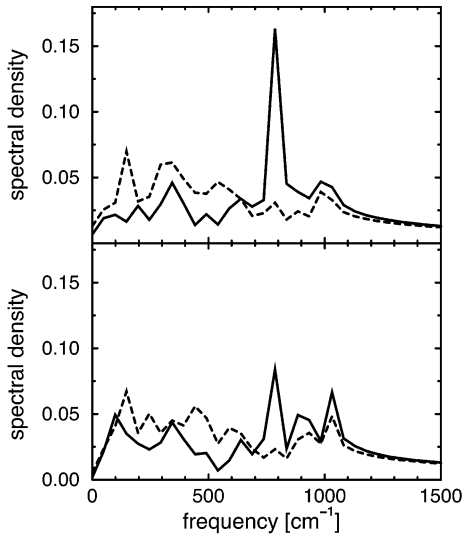

Figure 5. Power spectra of silicon (—) and oxygen (– –) in the clay layer for hydrated (top) and dry (bottom) clay systems.

whereas power spectra of velocity autocorrelations are usually a good first indication of IR absorption, the neglect of the frequency dependence of the electronic contribution to the intensity prevents direct comparison with experimental data. The IR activity of vibrational modes can vary wildly. The interpretation of line shapes in condensed-phase systems with a substantial degree of disorder, such as clays, is further complicated by inhomogeneous broadening.

It is not impossible, therefore, that a difference in the electronic response could be responsible for the experimentally observed structure in the wet clay spectrum. Moreover, the impressive track record of the DFT approach as applied here for aqueous systems (see section III) gives us some confidence in the vibrational dynamics. The question of line shape is therefore crucial in our view. Fortunately, it can be resolved since the density functional evaluation of the oscillator strength has recently become feasible thanks to the Berry phase formulation of electronic polarization developed by Vanderbilt and coworkers.[54] Using this method, good results have been obtained for the IR spectrum of liquid water.[55] This rather demanding calculation is currently in progress and will enable us to analyze our results in more detail.

V. Conclusions

Two results from our ab initio molecular dynamics simulations of the hydration in the sodium montmorillonite clay model stand out: The first is the strong preference for intersolvent hydrogen bonding with only weak and short-lived hydrogen bonds to the silicate surface. The second is the liquidlike relaxation dynamics of the solvent layer. The corresponding solvent structure was found to be very similar to predictions made by a previous model-based Monte Carlo study.[5] This finding is significant because, although generated by empirical means, the interaction model was capable of reproducing the experimental perpendicular expansion in response to an increase in water content with a (perhaps unexpected) high degree of accuracy. Passing this critical test confers definite credibility to the model. The agreement with the ab initio MD can therefore be seen as a confirmation of the DFT description. This lends further support to our observations regarding the dynamics, which because of severe limitations in the time scale available to ab initio MD were necessarily of a rather qualitative nature.

TABLE 2: Hydration Energies (kcal/mol) and Average Separation between the Sodium Ion and Water Oxygen in $Na^+(H_2O)_n$ Clusters at a Cutoff Radius for the Plane Wave Basis of 70 Ry

	hydration energy (kcal/mol)			$r(Na^+-O)$ (Å)	
n	TM	exptl[33]	BHS	TM	BHS
1	24.1	23.4	20.4	2.215	2.403
2	20.8	19.2	18.2	2.244	2.421
4	14.1	13.2	13.2	2.368	2.485

The ab initio approach did allow us, however, to take the coupling to dynamical fluctuations in the mineral layer into account. Our results suggest therefore that, because of not yet fully understood effects of the two-surface geometry in clays, enclosed water is prevented from freezing, even in quantities as small as a double layer. This observation is in qualitative agreement with experimental values for the effective diffusion coefficient of 2D water in a vermiculite clay,[20] which are only a factor of 2−3 lower than that for bulk water. An important question in this context is, of course, the role of the counterion. In a continuation of this study, we are therefore planning to replace sodium with potassium.

Acknowledgment. We thank Stephen Stackhouse for his contributions to this work. Neal Skipper is acknowledged for valuable discussions during the course of this work.

Appendix: Pseudopotentials

The Trouillier−Martins (TM) pseudopotentials (PP) for oxygen and hydrogen are identical to potentials employed in previous calculations of aqueous systems. Oxygen is represented by the sum of an l = s and an l = p term with a pseudoradius of $r_c = 1.05$ au for both channels, and hydrogen is represented by only a local *s* with $r_c = 0.5$ au. For silicon, we used a sum of l = s, p, d with pseudoradii of $r_c = 1.9$, 2.1, and 2.1 au, respectively. Al and Na potentials must be handled with some caution because of the overlap with the charge density of the core states. This complication, which is particularly serious for the cations, can be resolved by the use of a nonlinear core correction[52] or by including the outer core shells in the valence. In the present calculations, however, we followed a more direct approach and modeled the Al and Na cation by regular semilocal norm-conserving pseudopotentials similar to those for oxygen and silicon. Thus, for Al, we used a BHS-type PP[50,51] specified by a sum of l = s, p, d with pseudoradii of $r_c = 1.21$, 1.57, and 1.57 au, respectively. For Na, we used a TM potential with the sum of an l = s and an l = p term with a pseudoradius of $r_c = 0.98$ au for both channels.

For the sodium ion, this approximation is more critical than for Al. The reason is that the sodium cation, unlike the aluminum ions, is in direct contact with the solvent. The sodium potential was therefore tested by computing the hydration energy and average separation between the sodium ion and water oxygen in $Na^+(H_2O)_n$ clusters containing 1 to 4 water molecules. We compare the results using the 4s Na pseudopotentials generated according to Trouiller and Martins[27] (MT) and a semicore Bachelet, Hamann, and Schluter[50,51] (BHS) PP in Table 2 with 3s and 3p states treated as valence electrons. From Table 2, it appears that the Na TM pseudopotential gives better results for the average distance between the sodium ion and water oxygens than the BHS pseudopotential (experimental value = 2.25 Å). Also, the TM pseudopotential gives good results for the hydration energy[34] compared with experimental values.[33] This convinced us that the use of a TM PP for sodium is justified.

References and Notes

(1) Grim, R. E. *Applied Clay Mineralogy*; McGraw-Hill: New York, 1960.
(2) Skipper, N. T.; Refson, K.; McConnell, J. D. C. *J. Chem. Phys.* **1991**, *94*, 7434−7445.
(3) Delville, A. *Langmuir* **1992**, *8*, 1796−1805.
(4) Skipper, N. T.; Chang, F.-R. C.; Sposito, G. *Clays Clay Miner.* **1995**, *43*, 294.
(5) Boek, E. S.; Coveney, P. V.; Skipper, N. T. *J. Am. Chem. Soc.* **1995**, *117*, 12608−12617.
(6) Boek, E. S.; Coveney, P. V.; Skipper, N. T. *Langmuir* **1995**, *11*, 4629−4631.
(7) Chang, F.-R. C.; Skipper, N. T.; Sposito, G. *Langmuir* **1995**, *11*, 2734−2741.
(8) Chavez-Paez, M.; van Workum, K.; de Pablo, L.; de Pablo J. J. *J. Chem. Phys.* **2001**, *114*, 1405−1413.
(9) Hensen, E. J. M.; Tambach, T. J.; Bliek, A.; Smit, B. *J. Chem. Phys.* **2001**, *115*, 3322−3329.
(10) Newman, A. C. D. *Chemistry of Clays and Clay Minerals*; Mineralogical Society: London, 1987.
(11) Brindley, G. W.; Brown, G. *Crystal Structures of Clay Minerals and Their X-ray Identification*; Mineralogical Society: London, 1980; Chapter 3.
(12) Sposito, G.; Prost, R. *Chem. Rev.* **1982**, *82*, 553−573.
(13) Cases, J. M.; Bérend, I.; Besson, G.; François, M.; Uriot, J. P.; Thomas, F.; Poirier, J. E. *Langmuir* **1992**, *8*, 2730−2739.
(14) Boek, E. S.; Coveney, P. V.; Refson, K., submitted for publication.
(15) Delville, A. *J. Phys. Chem.* **1993**, *97*, 9703−9712.
(16) Boek, E. S.; Briels, W. J.; van Eerden J.; Feil, D. *J. Chem. Phys.* **1992**, *96*, 7010−7018.
(17) Stackhouse, S.; Coveney, P. V.; Sandré, E. *J. Am. Chem. Soc.* **2001**, *123*, 11764−11774.
(18) Car, R.; Parrinello, M. *Phys. Rev. Lett.* **1985**, *55*, 2471.
(19) Odelius, M.; Bernasconi, M.; Parrinello, M. *Phys. Rev. Lett.* **1997**, *78*, 2855.
(20) Swenson, J.; Bergman, R.; Howells, W. S. *J. Chem. Phys.* **2000**, *113*, 2873−2879.
(21) Skipper, N. T.; Soper, A. K.; McConnell, J. D. C. *J. Chem. Phys.* **1991**, *94*, 5751−5760.
(22) Shewring, N. I. E.; Jones, T. G. J.; Maitland, G.; Yarwood, J. *J. Colloid Interface Sci.* **1995**, *176*, 308−317.
(23) Sposito, G. *The Surface Chemistry of Soils*; Oxford University Press: New York, 1984.
(24) Strictly speaking, our clay model should be considered to be a beidellite rather than a montmorillonite.[10] Both montmorillonite and beidellite are members of the smectite family of 2:1 clay minerals.
(25) Becke, A. D. *Phys. Rev. A* **1988**, *38*, 3098−3100.
(26) Lee, C.; Yang, W.; Parr, R. G. *Phys. Rev. B* **1988**, *37*, 785−789.
(27) Troullier, N.; Martins, J. L. *Phys. Rev. B* **1991**, *43*, 1993.
(28) Sprik, M.; Hutter, J.; Parrinello, M. *J. Chem. Phys.* **1996**, *105*, 1142.
(29) Silvestrelli, P. L.; Parrinello, M. *J. Chem. Phys.* **1999**, *111*, 3572.
(30) Schwegler, E.; Galli, G.; Gygi, F.; Hood, R. Q. *Phys. Rev. Lett.* **2001**, *87*, 265501.
(31) All intermolecular interactions, other than electrostatic, strictly vanish in the GGA when molecular charge distributions no longer overlap. Long-range attraction in the form of the $1/r^6$ dispersion interaction is therefore not accounted for. However, for some GGAs such as BLYP, the short-range attraction resulting from the correlation energy of overlapping charge in dense liquids is able to compensate for the missing dispersion energy. This is one of the reasons for our preference for this functional.
(32) Lyubartsev, A. P.; Laasonen, K.; Laaksonen, A. *J. Chem. Phys.* **2001**, *114*, 3120.
(33) Ramaniah, L. M.; Bernasconi, M.; Parrinello, M. *J. Chem. Phys.* **1998**, *109*, 6839.
(34) Vuilleumier, R.; Sprik, M. *J. Chem. Phys.* **2001**, *115*, 3454−3468.
(35) Ramaniah L. M.; Bernasconi M.; Parrinello, M. *J. Chem. Phys.* **1999**, *111*, 1587.
(36) Marx, D.; Sprik, M.; Parrinello, M. *Chem. Phys. Lett.* **1997**, *273*, 360.
(37) Bako, I.; Hutter, J.; Palinkas, G. *J. Chem. Phys.* **2002**, *117*, 9838.
(38) Bruge, F.; Bernasconi, M.; Parrinello, M. *J. Am. Chem. Soc.* **1999**, *121*, 10833.
(39) Sillanpaa, A. J.; Paivarinta, J. T.; Hotokka, M. J.; Rosenholm, J. B.; Laasonen, K. E. *J. Phys. Chem. B* **2001**, *105*, 10111.
(40) Laasonen, K. E.; Klein, M. L. *J. Phys. Chem. A* **1997**, *101*, 98.
(41) Tobias, D. J.; Jungwirth, P.; Parrinello, M. *J. Chem. Phys.* **2001**, *114*, 7036.
(42) Ensing, B.; Meijer, E. J.; Blochl, P. E.; Baerends, E. J. *J. Phys. Chem. A* **2001**, *105*, 3300.
(43) Sillanpaa, A. J.; Simon, C.; Klein, M. L.; Laasonen, K. *J. Phys. Chem. B* **2002**, *106*, 11315.
(44) Odelius, M. *Phys. Rev. Lett.* **1999**, *82*, 3919−3922.
(45) Lindan, P. J. D.; Harrison, N. M.; Gillan, M. J. *Phys. Rev. Lett.* **1998**, *80*, 762−765.
(46) Stich, I.; Gale, J. D.; Terakura, K.; Payne, M. C. *J. Am. Chem. Soc.* **1999**, *121*, 3292−3302.
(47) Hutter, J.; Alavi, A.; Deutsch, T.; Bernasconi, M.; Goedecker, S.; Marx, D.; Tuckerman, M. and Parrinello, M. *CPMD* (Car−Parrinello molecular dynamics); MPI Solid State Research Institute, Stuttgart, Germany and the IBM Research Laboratory, Zürich, Switzerland
(48) Skipper, N. T.; Neilson, G. W. *J. Phys.: Condens. Mater.* **1989**, *1*, 4141.
(49) Slade, P. G.; Stone, P. A.; Radoslovich, E. W. *Clays Clay Miner.* **1985**, *33*, 51.
(50) Bachelet, G. B.; Hamann, D. R.; Schlüter, M. *Phys. Rev. B* **1982**, *26*, 4199.
(51) Hamann, D. R. *Phys. Rev. B* **1989**, *40*, 2980.
(52) Louie, S. G.; Froyen, S.; Cohen, M. L. *Phys. Rev. B* **1982**, *26*, 1738−1742.
(53) Sposito, G.; Prost, R.; Gaultier, J.-P. *Clays Clay Miner.* **1983**, *31*, 9−16.
(54) King-Smith, R. D.; Vanderbilt, D. *Phys. Rev. B* **1993**, *47*, 1651.
(55) Silvestrelli, P. L.; Bernasconi, M.; Parrinello, M. *Chem. Phys. Lett* **1997**, *277*, 478−482.